

INVESTIGATION OF THE SURFACE FATIGUE OF CARBIDE COMPOSITES AND PVD HARD COATINGS

Sergejev, F.; Antonov, M.; Gregor, A.; Hussainova, I.; Kulu, P. & Kübarsepp, J.

Abstract: *Surface fatigue testing have been carried out on a range of carbide composites and PVD (physical vapor deposition) hard coatings using an impact loading equipment. Results have confirmed the theoretical methodology of testing method by repeated loading of specimens with ball indenter of defined radius and constant maximum load. The precise prediction of surface fatigue life (N_f) for carbide composites has been done. An attempt of results interpretation is presented in order to predict the surface fatigue limit (σ_{sf}) of studied materials.*

The dramatic increase of plastically deformed zone dimensions under indent after high cycle fatigue is observed. The fractographical investigations of sub-surface layer of affected site revealed the specific mechanism of fatigue crack advancement.

Key words: surface fatigue; carbide composites; PVD coatings

1. INTRODUCTION

During cyclic loading the repeatable tribological contacts exist between working parts in bearings, gears, cams, machining tools and etc. Stressing in a changing mechanical strain during operation mainly causes so-called surface ruins - wear by impact or rolling [1]. Pitting of contact surfaces - phase transformations, surface cracking and crack propagation processes, are the traces of surface fatigue.

Surface fatigue testing is an essential tool for assessment of properties of materials and coatings [2] working under complex loading conditions.

The high cycling testing is costly and time consuming this is why the information concerning the contact fatigue properties for many materials is not available in published literature.

2. TESTING PROCEDURE AND MATERIALS

Tests were performed on the surface fatigue tester designed and developed in the Laboratory of Tribology, Tallinn University of Technology.

2.1 Surface fatigue tester

The dynamic load (up to 600 N) in test rig is transferred from the hammer that is connected to, and accelerated by the rotating disk, see Fig. 1. The transferred energy depends on the speed and mass of hammer and can be adjusted as needed. Several hammers (max. number is 12 pcs.) fastened on the periphery of the disk allow increasing the frequency at least up to 100 Hz. The affordable frequency of the impact is higher than that of hydraulic or electromagnetic testers and the energy is higher than that of pneumatic ones [1-4].

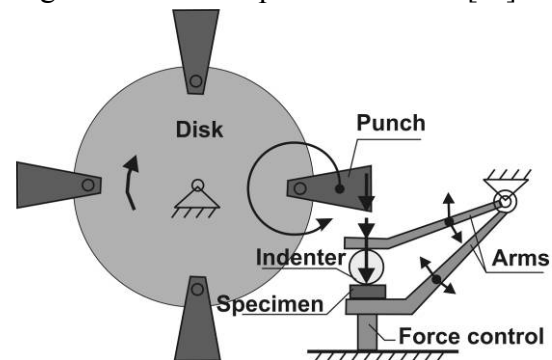


Fig. 1. The schematic representation of the testing apparatus.

To minimize the wear of moving parts and its effect on the change of contact conditions during testing the arm type construction was applied. The applied force measurement system (force sensor) and the protection in case of the overload are used for monitoring of the contact parameters.

It is possible to use large size indenters (with diameter of 10-30 mm) in order to reproduce closest to the flat-flat surface contact conditions.

The resulting force F (N) of impact loading can be equated as [5]:

$$F = V \cdot m \cdot f, \quad (1)$$

where V – speed, m/s;

m – mass, kg;

f – frequency of loading, Hz.

The force measured during the tests was slightly higher (by ~10 %) than that equated according to tests conditions because the real point of impact was located closer to the centre of the disk (centre of the mass of the hammer).

Tests were performed with use of indenters made of hardmetal (WC-6 wt% Co) with diameter of 12.0 mm.

All experiments were conducted in air at room temperature (20 ± 2 °C) with a relative humidity (RH) of 45 ± 5 pct.

2.2 Carbide composites

Two different grades were selected for testing as they are wear resistant composites prospective (grade T70/14) and conventionally used (grade H15) as metalforming tool materials [6-8].

Specimens, plates with dimensions of $23 \times 15 \times 5$ mm³, were produced through conventional press and sinter powder metallurgy routine by Laboratory of Powder Metallurgy of Tallinn University of Technology (according to ASTM B406). Test specimens were grinded and polished to the surface roughness of $R_a = 0.2$ μm.

Composition, microstructural parameters and main mechanical properties of tested WC- and TiC-based carbide composites are listed in Table 1.

Table 1. Main characteristics of tested carbide composites

Grade	Composition, wt%	Average grain size, μm	Transverse rupture strength R_{Tz} , MPa	Vickers hardness HV
H15	85 WC+15 Co	2.0	2900	1170
T70/14	70 TiC+Fe/14 Ni	2.2	2110	1270

The microstructures of investigated WC-Co and TiC-Fe/Ni composites are presented in Fig. 2. There is a distinct difference in the shapes of carbide grains as TiC-grains are more spherical (rounded) compared with the angular shape of tungsten carbide. On a closer examination a core-rim structure of TiC-grains can be observed [9,10].

The impacting frequency was equal to 50 Hz. Tests were limited by the maximum number of 0.5×10^6 cycles of loading (N).

The resulting force F was equal to 3.5 N (180 mJ per impact).

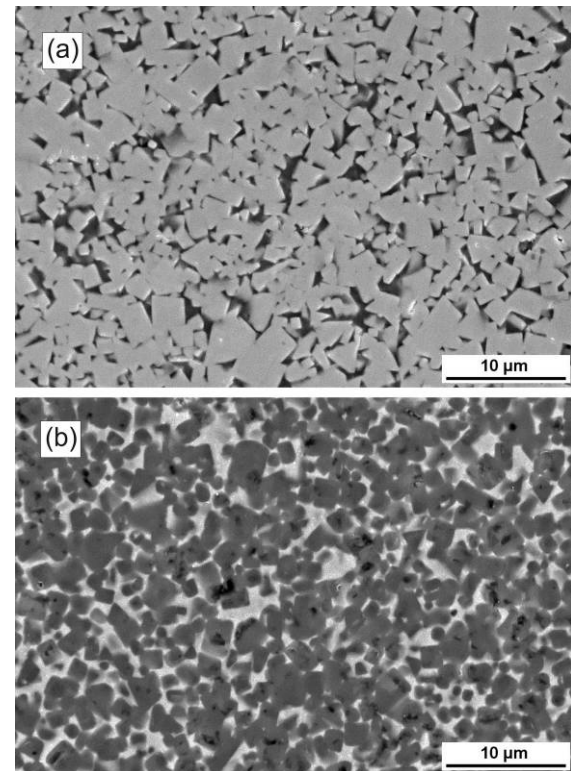


Fig. 2. SEM micrographs of tested (a) H15 and (b) T70/14 carbide composites.

2.3 Hard PVD coatings

Three different substrate materials were used for the deposition of PVD coatings – the hotworking steel Weartec SF, Vanadis 6 and steel C45. Weartec SF was hardened to the hardness value of 64 HRC. Vanadis 6 and C45 were untreated and had a hardness of 25-30 HRC.

After diamond polishing ($R_a=0.2 \mu\text{m}$) all samples ($23 \times 23 \times 5 \text{ mm}^3$ plates) were degreased ultrasonically in phosphate-alkali solution, rinsed in ethanol and dried in air.

Five different coatings: monolayers (TiAlN); gradient (TiN, TiCN and AlTiN) and nanostructured coating (nc-(AlTi)N/a-Si₃N₄) were deposited using an arc ion plating technique in a PVD plant Platit π -80. The thicknesses of all deposited coatings were 2.3 μm . Main characteristics of tested PVD coatings can be found from Table 2.

All samples were heated up to a temperature of 450°C in a vacuum chamber and kept there for a one hour. A high vacuum (better than 10^{-4} mbar or 10^{-5} kPa) was achieved (measured with the Baratron and Pirani vacuum gauges). Then all samples were cleaned in a pulsed argon (Ar) glow discharge at 425 °C, with a bias of -850 V at pressure of 4×10^{-3} mbar (4×10^{-4} kPa) to reduce contaminants and oxides on the surfaces of the samples. Titanium cathode was cleaned in an Ar plasma at arc current of 60 A. After that a thin metallic Ti layer (Ti etching) was deposited in an Ar environment at a temperature of 430 °C, at same conditions.

Table 2. Main properties of tested PVD coatings [11]

Name	Nanohardness, GPa	Friction coefficient	Max. usage temperature, °C
TiN	24	0.55	600
TiCN	37	0.20	400
TiAlN	35	0.50	800
AlTiN	38	0.70	900
nACo®	40	0.45	1100

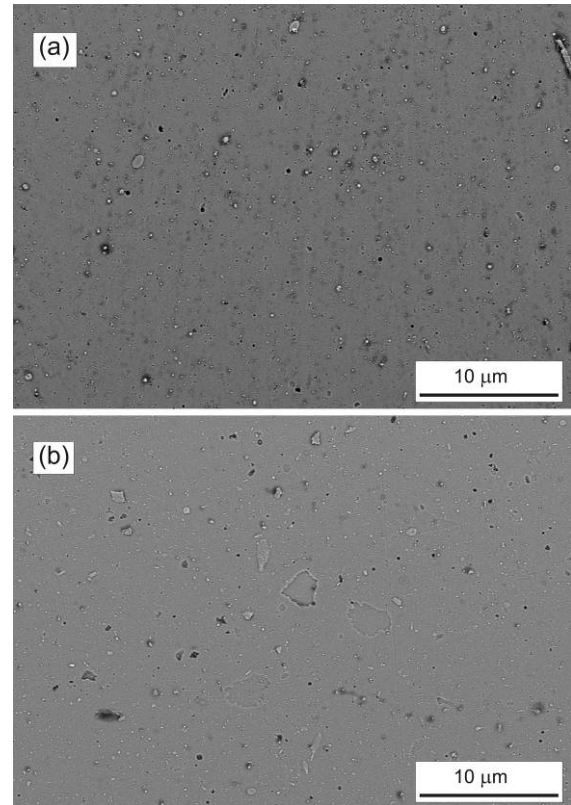


Fig. 3. SEM micrographs of tested PVD coatings: (a) TiN and (b) nACo®.

During this step Ti cathode arc current was reduced to value of 52 A. Later on the substrate bias voltage was increased to a value of -900 to -1000 V to create a valuable adhesion layer on a surface of the substrate.

Fig. 3 shows the microstructures only of TiN and nACo® (nc-(AlTi)N/a-Si₃N₄) coatings, as the appearance of all investigated coatings before testing is very similar.

The testing impacting frequency for PVD coatings was equal to 12.5 (only untreated substrate), 18.75 (only treated substrate, weight of hammers is doubled) and 25.0 Hz. Tests were limited by the maximum number of 10^4 cycles of loading.

The resulting force F for different testing regimes for PVD coatings according to various substrate types used was equal to 1.1 N (14 mJ per impact at 12.5 Hz), 1.2 N (65 mJ per impact at 18.75 Hz) and 0.3 N (58 mJ per impact at 25.0 Hz). The effect of substrate treatment on the properties of coatings was investigated.

3. RESULTS AND DISCUSSION

3.1 Carbide composites

The prediction of surface fatigue life (N_f – number of cycles till failure) for carbide composites can be done using Eq. [12]:

$$N_{fs} = \frac{E \cdot E_i}{0.25 \cdot (1 - \nu^2) \cdot \sigma_0^2 \cdot \sqrt{\pi \cdot \text{area}}}, \quad (2)$$

where E – Young's modulus, GPa;
 E_i – total accumulated energy, J;
 ν – Poisson's modulus;
 σ_0 – tensile/compressive stress, GPa;
 area – maximum area of structural defect, mm^2 .

Results of surface fatigue testing can be presented in the form of indent scar dimension versus number of loading cycles (logarithmic scale) plot, see Fig. 4.

Titanium carbide based cermet appears to have smallest diameters of indents after applied number of loading cycles (max. 0.5×10^6) among tested materials.

Fractographical investigation showed that in the centre of indent the binder is almost totally absent (see Figs. 5 and 6). The exposed pores on the periphery are filled up with extruded binder and separated/fractured carbide grains, which corresponds to [4,13].

In the case of TiC-based cermet the extruded binder volume is much larger (see Fig. 6) if compare with WC-based hardmetal. Binder forms the layered struc-

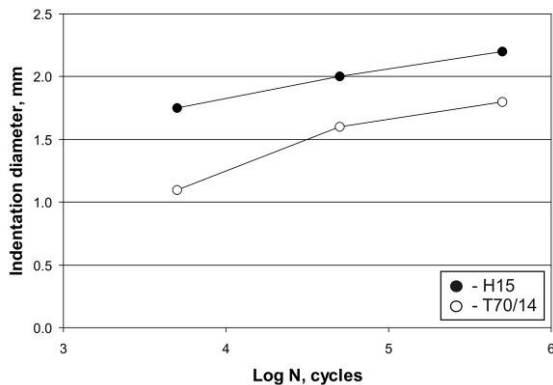


Fig. 4. Indentation diameter as a function of the number of loading cycles for tested carbide composites.

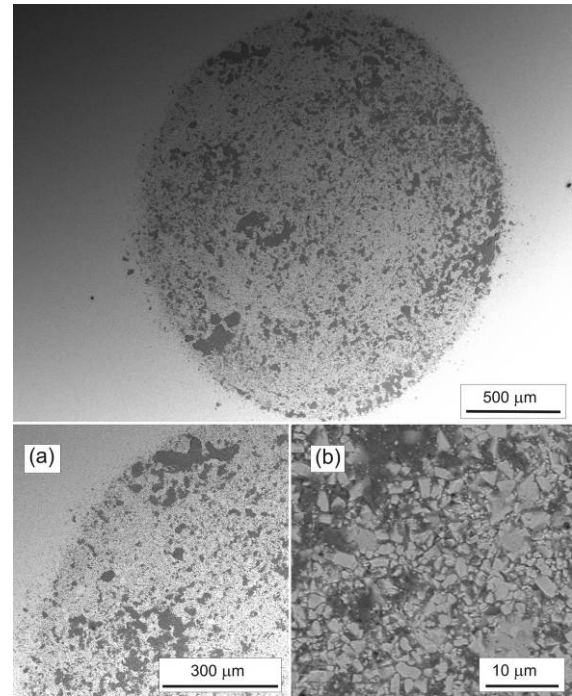


Fig. 5. SEM images of WC-15 wt% Co hardmetal surface after loading of 0.5×10^6 cycles: (a) the edge of indent and (b) the centre of indent.

tures which act as protection of the brittle carbide surface from further degradation during loading that leads to the better wear properties of the surface.

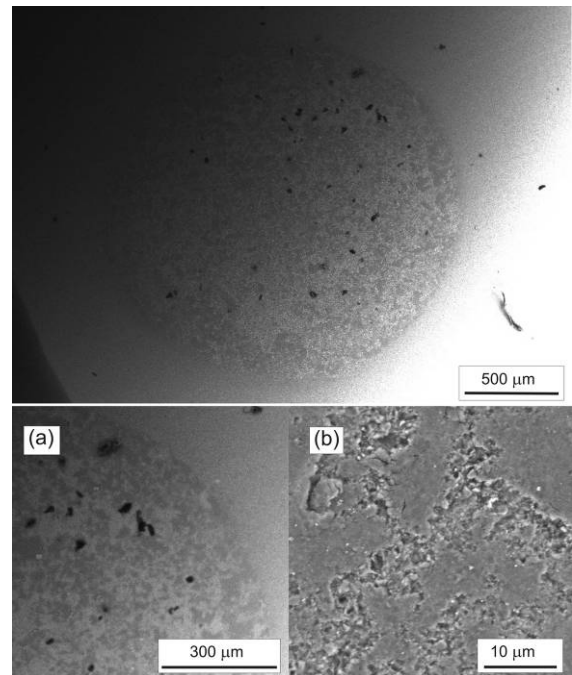


Fig. 6. SEM images of TiC-Fe/14 wt% Ni cermet surface after loading of 0.5×10^6 cycles: (a) the edge of indent and (b) the centre of indent.

3.2 PVD hard coatings

Unfortunately we are not able to predict the surface fatigue life of hard PVD coatings as main mechanical characteristics needed for calculation (see Eq. 2) are not available yet. Though the fractographical examination of the coatings surfaces after cyclic loading exposed same failure mechanisms as published previously [1,2,14]. We have compared failure behaviour of coatings depending on the substrate treatment and testing regimes (frequency and impulse change). Tested coatings on untreated substrate showed straight dependence on the loading frequency. The indent diameter decreased proportionally (about two times) with frequency reduction (see Figs. 7a and 8a). On contrary no changes in indent dimensions and fracture behaviour can be observed for coatings on

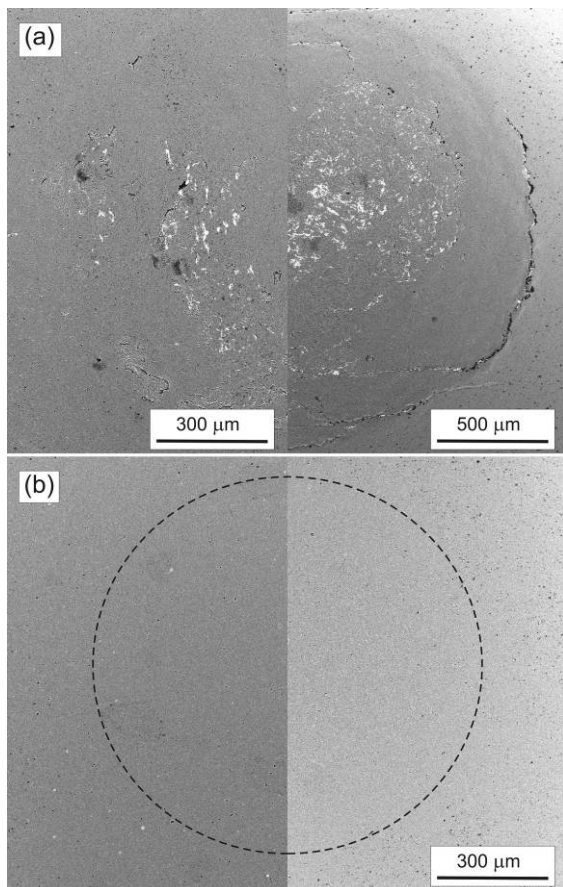


Fig. 7. Fractographs of indents for TiCN coating: (a) untreated substrate (left – 12.5 Hz, right – 25.0 Hz); (b) treated substrate (left – 18.75 Hz, right – 25.0 Hz).

treated substrate (see Figs. 7b and 8b) as the transferred energy rate was not changed (~60 mJ/impact).

Largest indent dimensions (diameter of 1.5 mm) are marked in the case of TiN coating. For other coatings those are about ~1 mm for all tested coating materials.

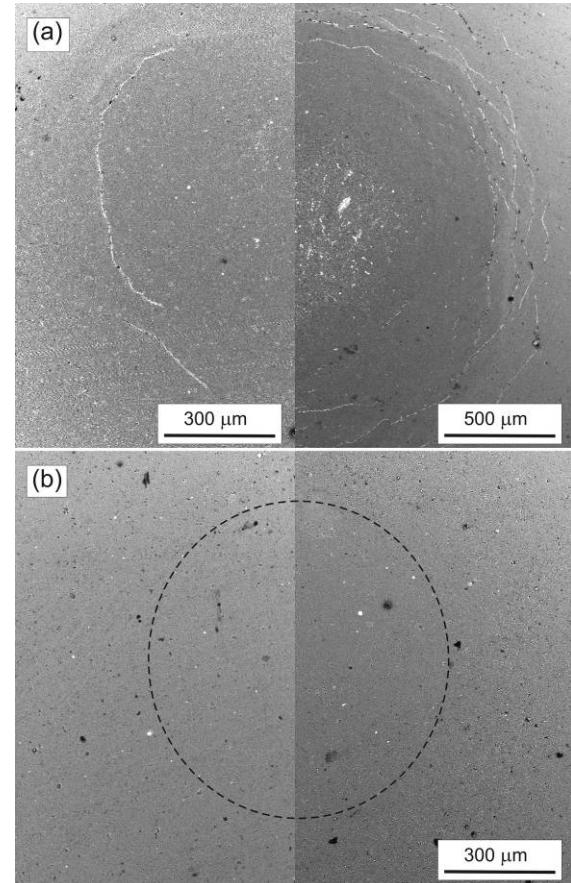


Fig. 8. Fractographs of indents for AlTiN coating: (a) untreated substrate (left – 12.5 Hz, right – 25.0 Hz); (b) treated substrate (left – 18.75 Hz, right – 25.0 Hz).

4. CONCLUSIONS

Severe fatigue degradations of tested carbide composites (TiC- and WC-based) and hard PVD coatings (TiN, TiCN, TiAlN, AlTiN and nACo®) are observed. The increase of plastically deformed zone dimensions under indent after cycle fatigue loading (10^4 cycles for PVD coatings and 0.5×10^6 for carbide composites) was shown. Change of impact frequency has no effect on the surface fatigue behaviour of material if impulse remains the same.

Further investigations are to be performed to clarify peculiarities of surface fatigue of carbide composites and coatings.

ACKNOWLEDGEMENTS

This research was supported by the Estonian Ministry of Education and Science (SF Projects - SF0140062s08 and SF0140091s08) and the Estonian Science Foundation (grant No. 6163).

5. REFERENCES

1. Lugscheider, E., Knotek, O., Wolff, C., Bärwulf, S. Structure and properties of PVD-coatings by means of impact tester. *Surf. Coat. Tech.*, 1999, **116–119**, 141–146.
2. Bouzakis, K.-D., Asimakopoulos, A., Michailidis, N., Kompogiannis, S., Maliaris, G., Giannopoulos, G., Pavlidou, E., Erkens, G. The inclined impact test, an efficient method to characterize coatings cohesion and adhesion properties. *Thin Solid Films*, 2004, **469–470**, 254–262
3. Sekkal, C., Langlade, C., Vannes, A. B. Tribologically transformed structure of titanium alloy (TiAl6V4) in surface fatigue induced by repeated impacts. *Mat. Sci. Eng. A-Struct.*, 2005, **393**, 140–146..
4. Guillou, M. O., Henshall, J. L., Hooper, R. M. The measurement of surface contact fatigue and its application to engineering ceramics. *Mat. Sci. Eng. A-Struct.*, 1996, **209**, 116-127.
5. Jones, F. D., Horton, H. L., Ryffel, H. H., Oberg, E. *Machinery's Handbook - 27th ed.* Industrial Press, New York, 2004.
6. Klaasen, H., Kübarsepp, J., Eigi, R. Peculiarities of hardmetals wear in blanking of sheet metals. *Tribol. Int.*, 2006, **39**, 303–309.
7. Kübarsepp, J., Klaasen, H., Pirso, J. Behaviour of TiC-base cermets in different wear conditions. *Wear*, 2001, **249**, 229–234.
8. Kübarsepp, J., Klaasen, H., Sergejev, F. Performance of Cemented Carbides in

Cyclic Loading Wear Conditions. *Materials Science Forum*, 2007, **534–536**, 1221-1224.

9. Hussainova, I. Effect of micro-structure on the erosive wear of titanium carbide-based cermets. *Wear*, 2003, **255**, 121–128.
10. Kollo, L., Volobujeva, O. Reactive sintering of (Ti,W)C-Ni and TiCFeNiSi cermets from high-energy milled powders. In: *Proceedings of Euro PM 2007 Congress & Exhibition*, Toulouse, France, 14-17 Oct. 2007, **1**, 227 – 231.
11. Platit® Homepage - Coating Guide, <http://platit.com/coating-guide> (last access date 03.03.2008).
12. Sergejev, F., Preis, I., Kübarsepp, J., Antonov, M. Correlation between surface fatigue and microstructural defects of cemented carbides. *Wear*, 2008, **264**, 770-774.
13. Terheci, M. Wear by surface fatigue on a new foundation Part II. Particle detachment mechanisms and quantitative aspects. *Wear*, 1998, **218**, 191-202.
14. Bouzakis, K.-D., Siganos, A., Leyendecker, T., Erkens G. Thin hard coatings fracture propagation during the impact test. *Thin Solid Films*, 2004, **460**, 181–189.

6. DATA ABOUT AUTHORS

Name(s), address(es), contact data:

Fjodor Sergejev, 19086 Tallinn, Ehitajate tee 5, Estonia, Fjodor.Sergejev@ttu.ee, +372 6203354;

Maksim Antonov, 19086 Tallinn, Ehitajate tee 5, Estonia, Maksim.Antonov@ttu.ee, +372 6203355;

Andre Gregor, 19086 Tallinn, Ehitajate tee 5, Estonia, Andre.Gregor@ttu.ee, +372 6203371;

Irina Hussainova, 19086 Tallinn, Ehitajate tee 5, Estonia, irhus@staff.ttu.ee, +372 6203355;

Priit Kulu, 19086 Tallinn, Ehitajate tee 5, Estonia, Priit.Kulu@ttu.ee, +372 6203352;

Jakob Kübarsepp, 19086 Tallinn, Ehitajate tee 5, Estonia, jakob@staff.ttu.ee, +372 6202006.